Theranostic Nanoparticles Loaded with Imaging Probes and Rubrocurcumin for Combined Cancer Therapy by Folate Receptor Targeting

UNIVERSITÀ DEGLI STUDI DI TORINO

“Theranostic” nanoparticles loaded with imaging probes and rubrocurcumin for a combined cancer therapy.

Diego Alberti[a], Nicoletta Protti[b], Morgane Franck[a], Rachele Stefania[a], Silva Bortolussi[b], Saverio Altieri[b], Annamaria Deagostino[c], Silvio Aime[a], Simonetta Geninatti Crich*[a]

[a] Dr D. Alberti, Dr. Morgane Frank, Dr. R. Stefania, prof S. Aime, prof S. Geninatti Crich, Department of Molecular Biotechnology and Health Sciences; University of Torino, via Nizza 52, 10126, Torino, Italy. E-mail: simonetta.geninatti@unito.it; ORCID ID: http://orcid.org/0000-0003-2998-5424

[b] Dr. N. Protti, Dr. S. Bortolussi, prof. S. Altieri, Department of Physic, University of Pavia, via Bassi 6, 27100, Pavia, Italy; Nuclear Physics National Institute (INFN), Unit of Pavia, via Bassi 6, 27100, Pavia, Italy.

[c] Prof. A Deagostino, Department of Chemistry, University of Torino,via P. Giuria 7, 10125, Torino, Italy.

Supporting information for this article is given via a link at the end of the document.

Abstract The combination of different therapeutic modalities is a promising option to combat tumour recurrence. PolyLactic and Glycolic Acid nanoparticles are exploited for the simultaneous delivery of a boron-curcumin complex (RbCur) and an amphiphilic Gd complex into tumour cells with the aim of performing Boron and Gadolinium Neutron Capture Therapy (NCT) in combination with an additional curcumin anti-proliferative effect. Furthermore, the use of Gd complexes allows the MRI assessment of the amount of B and Gd internalized by tumour cells. PLGA nanoparticles are targeted to ovarian cancer cells (IGROV-1), by including in the formulation a pegylated phospholipid functionalized with the folate moiety. NCT is performed on IGROV-1 cells internalizing 6.4 and 78.6 μg/g of ^{10}B and ^{157}Gd, respectively. The synergic action of neutron treatment and curcumin cytotoxicity results in a significant therapeutic improvement.

Introduction

In recent years, much attention has been devoted to the use of combinations of different therapeutic modalities, as possible strategies to treat cancer.[1] This relies on the evidence that although a large majority of chemotherapeutic protocols and radiotherapies can considerably reduce tumour masses, they often fail in causing their complete regression as shown by a high number of tumour recurrence cases.[2] Moreover, the time-dependent development of chemoresistance and radioresistance by a minor cell population within the tumour and the nonspecific toxicity toward normal cells are the other major limitations of standard therapies.[2-3] There is now an approved view that complete tumour regression can be achieved by the combination of different therapeutic strategies whereas a reduction in the off target toxicity can be tackled by developing target-specific drugs endowed with reduced adverse effects or by using a more specific radiotherapeutic protocol able to discriminate between healthy and cancer cells.

Boron Neutron Capture Therapy (BNCT) is a non-conventional radiotherapy that combines low energy neutron irradiation with the presence of boron-containing compound at the targeted cells. Neutrons are captured by nonradioactive isotope ^{10}B that disintegrates into alpha particles and lithium nuclei that cause non reparable damage to the cell where they were generated.[4] The low range of the charged particles permits the selective damage of tumour cells without affecting adjacent healthy cells if ^{10}B atoms are selectively accumulated in the intracellular space of tumour cells. This makes BNCT a promising option for the treatment of infiltrating tumours and disseminated metastases that cannot be treated by methods requiring a precise localization of the mass, such as surgery or conventional radiotherapy.[5] It has been estimated that approximately 10-30 μg of ^{10}B per gram of tumour mass are needed to deliver therapeutic dose of radiation to the tumour mass using an irradiation time shorter than a hour which allows not to exceed the tolerance dose in normal tissues.[6] The delivery of boron should be as selective as possible to tumour in order to increase the amount of internalized B in neoplastic cells and at the same time to minimize uptake in surrounding healthy tissues and permanence in blood which could create damages to normal organs and vessels. Currently, two BNCT drugs are available for clinical investigation namely: i) L-paraboronophenylalanine (BPA), that has been used in clinical trials to treat glioblastoma,[7] head and neck recurrent cancer [8] and melanoma [9] and ii) sodium mercaptoundecahydro-closo-dodecaborate (BSH) that has been investigated for the treatment of malignant glioma.[10] Despite their clinical use, both BPA and BSH show low cell targeting selectivity and great efforts have been made by several research groups to develop new and more selective boron delivery agents.[11]

In this study, the stable adduct formed by boric acid, curcumin and oxalic acid (Rubrocurcumin)[12] has been exploited to combine BNCT with the anti-cancer activity of curcumin. Curcumin is a natural polyphenolic compound showing a wide range of pharmacological activities.[13] It has been proposed as therapeutic agent as it showed antitumour activity *in vitro* and in animal models through the modulation or inhibition of multiple molecular pathways.[14] Furthermore, it has been recently reported that curcumin acts as an efficient radiosensitizer due the upregulation of genes responsible for cell death.[15] Another important property is that, unlike other known chemotherapeutic compounds, curcumin does not cause any damage to the normal cells[16] and, in some cases, curcumin has also been shown to protect normal organs such as liver, kidney, oral mucosa, and heart from chemotherapy and radiotherapy-induced toxicity.[15] The formation of stable red complexes between B and curcumin has been exploited for the spectrophotometric detection of trace amount of B in various media, including biological materials (e.g. food-stuff, plants and blood plasma), natural water and sea water, soil, iron and steel, as well as material relevant to nuclear technology.[17] Moreover, promising medicinal applications of metal curcumin complexes have been reported.[18] The factor that limits the use of free curcumin and its complexes for tumour therapy is its low solubility in water, which in turn limits its bioavailability when administered orally. To this purpose, nanotechnology-based carriers[19] have been recently proposed for selective delivery to

tumour sites along with appropriate curcumin functionalization for example with PEG chains.[20]

Poly (lactic-co-glycolic acid) (PLGA) is one of the most effective biodegradable polymeric nanoparticles (NPs). It has been approved by the US FDA as drug delivery system due to its controlled and sustained-release properties, low toxicity, and biocompatibility with tissue and cells.[21] In this study, curcumin-boron complexes (RbCur) have been loaded into folate-targeted PLGA nanoparticles (PLGA-NP-Folate)(Figure 1) together with an amphiphilic Gd based Magnetic Resonance Imaging (MRI) contrast agent (Gd-DOTAMA).[22]

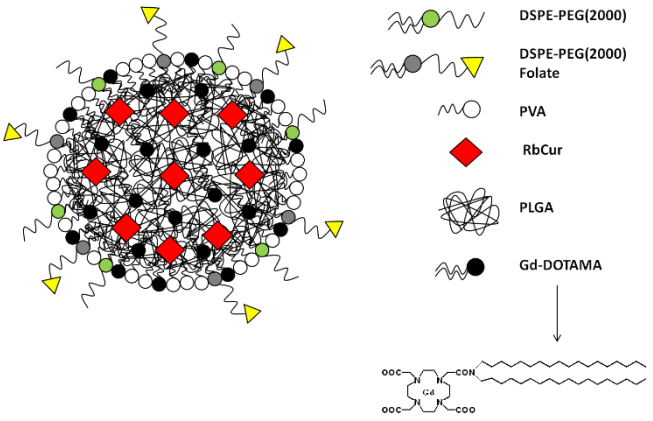

Figure 1: Schematic representation of folate conjugated PLGA RbCur/Gd nanoparticles (PLGA-NP-Folate)

This novel theranostic agent allows i) to maximize the selective uptake of B atoms from tumour cells by targeting folate receptors alpha (FRA) and ii) to quantify B distribution in the tumour and in other tissues indirectly by means of MRI response. To date a non-invasive and repeatable *in vivo* B detection method is not available, even if it is well established that the measurement of local B concentration is crucial to determine the optimal neutron irradiation time, to calculate the delivered radiation dose and to evaluate the best irradiation time and duration.[23] Moreover, ^{157}Gd is the second most studied element to perform NCT, as a consequence of its high cross section for the capture of low-energy neutrons. The biological efficacy of Gd-based NCT is mainly due to the Auger electron cascade induced by the internal conversion process that occur in competition with the gamma-ray emission upon the neutron capture reaction from the ^{157}Gd isotope. The energy associated to the Auger electrons is 0.6% of the total emitted energy (7.94 MeV). Despite the low energy these electrons may give strong cytotoxic effects when the ^{157}Gds are very close to the cellular DNA. [5,24] In addition, Gd neutron capture results also in a release of long range γ–rays which can be advantageous to damage also resistant cells not internalizing enough B/Gd to perform an effective therapy.[25] In this particular case, the location of the element is not critical with regard to target cell due to their longer ranges. Having BNCT and Gd-NCT different mechanisms of action, one expects advantages from their combined use. [26] One straightforward route dealt with the simultaneous administration of two NCT agents, one carrying ^{10}B, the other ^{157}Gd, but this approach has the disadvantage that their uptake and distribution within the tumour may be quite different. In this study, ^{10}B and ^{157}Gd are loaded in the same nanoparticle thus permitting their simultaneous distribution. The eventual increment of the dose due to the ^{157}Gd capture reaction is herein analysed and discussed.

Results and Discussion

Synthesis of the Boron/Curcumin dual agent Rubrocurcumin (RbCur) (Figure 2) has been performed by reacting boric acid, curcumin and oxalic acid according to the procedure described by Sui Z et al.[12] The complex has been characterized by UV-VIS spectrophotometry and by ^{1}H-NMR. Figure 3 shows that after the complex formation, the curcumin peak at 430nm in the parent compound is shifted to 545nm, where RbCur exhibits its maximum characteristic peak in ethanol.

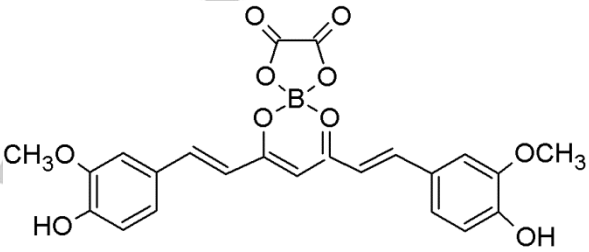

Figure 2: Schematic representation of Rubrocurcumin (RbCur).

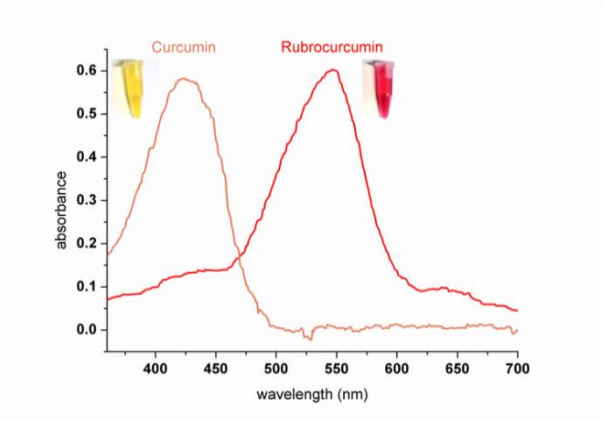

Figure 3: UV-VIS spectra of curcumin and Rubrocurcumin acquired in ethanol at 10 µM concentration.

Synthesis of PLGA nanoparticles

The methodology to obtain Folate conjugated and non-conjugated PLGA nanoparticles (PLGA-NP-Folate and PLGA-NP-Ctrl, respectively) was based on the o/w emulsion solvent extraction method.[21] The organic phase was prepared dissolving PLGA RG 503H, RbCur, Gd-DOTAMA, pegylated phospholipid (DSPE-PEG(2000)methoxy) in 9:1 chloroform: methanol. For the preparation of PLGA-NP-Folate DSPE-PEG(2000)Folate was added to the organic phase. The water phase consisted of a poly(vinyl alcohol) (PVA) aqueous solution (3% w/v). PVA is the most commonly used emulsifier for the preparation of these PLGA based NP because it yields particles that are relatively uniform, small sized, and easy to be re-dispersed in water.[27] To obtain PLGA nanoparticles, the organic phase was added to the aqueous phase and the mixture was sonicated for 5 minutes. Then, the solidification of nanospheres was obtained by organic solvent evaporation from the o/w emulsion. The organic solvent was slowly removed under vacuum in a rotary evaporator (2.5 h).

Table 1: Encapsulation yields of the RbCur and Gd-DOTAMA in PLGA-NP-Ctrl and PLGA-NP-Folate are reported together with their size (nm), their relaxivity ($mM^{-1}sec^{-1}$ 21.5 MHz 25°C) and their polydispersity index (PDI).

PLGA NP	Encapsulation yield (%) Gd-DOTAMA	RbCur	Relaxivity ($mM^{-1}sec^{-1}$)	Size (nm)	PDI
Ctrl	71 ± 7	12.6 ± 4.3	26.1±1.7	144±3	0.099
Folate	73 ± 15	10.4 ± 2.8	27.8±1.7	149±3	0.138

As reported in Table 1, the average hydrodynamic diameters of folate targeted and un-targeted PLGA nanoparticles obtained by dynamic light scattering (DLS) measurements show a homogeneous particle size distribution, of about 150 nm, with a polydispersity index (PDI) < 0.2. The encapsulation yields of Gd-DOTAMA were significantly higher than RbCur. An additional amount of curcumin (equal to the 43% w/w of the loaded RbCur) was found in the PLGA-NPs due to the partial dissociation of the RbCur complex, during the loading protocol, as shown in the UV-VIS spectrum acquired immediately after its preparation (Figure 4). However, the remaining RbCur complex encapsulated in the PLGA-NP was stable at 4°C for 2 weeks and all the following experiments were performed within this time. The Gd complexes incorporated in PLGA-NP endowed the system with a high relaxivity (26-28 $mM^{-1}sec^{-1}$ at 21.5 MHz, 25°C) as a consequence of the partial exposition of the hydrophilic portion of the complex to the particle external surface and the partial water diffusion inside the polymeric material that is inversely proportional to the PLGA-NP size.[28]

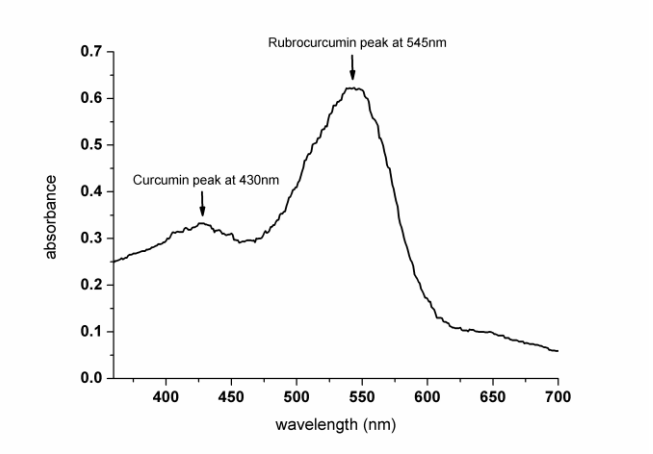

Figure 4: UV-VIS spectrum of RbCur loaded in PLGA-NP-Ctrl acquired in ethanol.

Stability of PLGA nanoparticles. The stability of PLGA nanoparticles was evaluated measuring by ICP-MS the release of B and Gd-DOTAMA from PLGA-NP-Ctrl and PLGA-NP-Folate. To this purpose, freshly prepared nanoparticle suspensions were dialyzed at 37°C against 40mL of HBS buffer for 5 days. Figure 5 shows that the amount of B released is about the 50% after 6h and it increased to 60% after 24 hours. In general, drug release depends upon: i) solubility, diffusion and biodegradation of the matrix materials; ii) loading efficiency of the drug and iii) size of the nanoparticles.[29] The faster B release from the NP herein observed is the consequence of the relatively low stability of RbCur at 37°C with the consequent release of boric acid. The longitudinal water proton relaxation rate (R_1) measured over 5 days (Figure 5) showed only minor changes, suggesting a negligible release of Gd-DOTAMA over the observed time period. The relatively fast release of B from the nanocage forced us to maintain short incubation time (6h) in the cell uptake experiments described in the following paragraph.

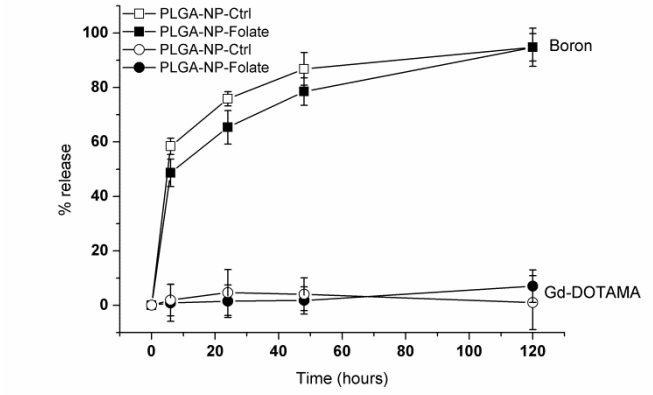

Figure 5: Evaluation of the stability of PLGA-NP-Ctrl and PLGA-NP-Folate loaded with RbCur and Gd-DOTAMA by measuring B and Gd concentrations in the NP solution over 5 days of dialysis at 37°C in HBS.

Folate targeting efficiency of PLGA-NPs and MRI visualization.

Folate-conjugated PLGA-NP have been tested for their efficacy in targeting Human Ovarian Cancer Cells (IGROV-1) overexpressing FRA.[30] Folic acid is a typical cell-targeting agent, because of its high affinity for FRA that is known to be overexpressed on the surface of many human cancer cells [31] and capture FA from the extracellular milieu and transport it inside the cell via a receptor-mediated endocytosis. There are different hypothesis concerning the precise mechanism of FR trafficking into cells. As reported by Stella *et al.* [32] and Lu *et al*, [32], folate-conjugated nanoparticles represent a multivalent form of the ligand folic acid. Since FRA are often disposed in clusters, conjugated nanoparticles could display a multivalent stronger interaction with the receptors and they can't be displaced by free folic acid.

Gd and B moles internalized by IGROV-1 cells, measured by ICP-MS after 6h incubation in the presence of increased concentration of PLGA-Folate nanoparticles were compared with those obtained using non-targeted ones. Figure 6 shows that Folate targeted NP reach a complete saturation when their concentration in the incubation medium was higher than 100 μM in Gd. This demonstrates a high affinity of Folate-targeted NP for the FRA and a negligible non-specific cell binding of non-targeted NP. The results obtained with IGROV-1 cells were compared with those obtained with human breast cancer cells (MCF-7) don't expressing FRA[32], with healthy mammary gland mouse cells (NMuMg) and embryo fibroblast cells (BALB/C 3T3) using the same incubation protocol. Figure 6 shows that the internalization of PLGA-NP-Folate by MCF-7, NMuMg and 3T3 is negligible in the range of the concentrations considered. These observations suggested that the selectivity of the PLGA-NP-Folate is directed only to tumour cells overexpressing FRA and that their targeted intracellular delivery takes place via a folate receptor mediated endocytosis mechanism.

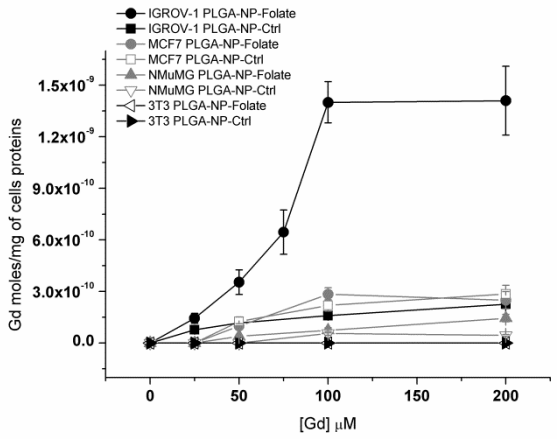

Figure 6: Uptake of PLGA-NP-Ctrl and PLGA-NP-Folate by IGROV-1, MCF-7, NMuMg and 3T3. Cells were incubated 6 hours at 37°C in the presence of increasing concentrations of PLGA-NP-Ctrl and PLGA-NP-Folate (25 – 200 μM Gd). The amount of Gd taken-up by cells has been determined by ICP-MS and it was normalized to the total cell protein content determined by the Bradford assay.

The amount of B and Gd internalized by IGROV-1 cells incubated with PLGA-NP-Folate (100 μM Gd), measured by ICP-MS, was of 6.4 and 78.6 μg/g of B and Gd, respectively. Finally, MRI images were acquired after incubating PLGA nanoparticles on IGROV-1 cells at a concentration of 100μM Gd. As shown in Figure 7, the T_1 weighted MR image acquired at 7 T of a phantom made of glass capillaries containing cell pellets, the recorded signal intensity (SI) of PLGA-NP-Folate in IGROV-1 cells was significantly higher with respect to non-targeted one. This observation confirms the specific accumulation of folate targeted NP in tumour cells with respect to control NP.

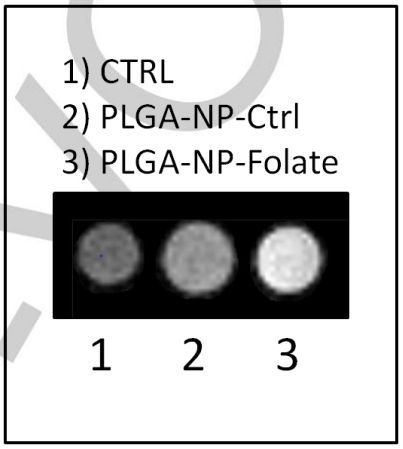

Figure 7: T_1-weighted spin echo MRI image (measured at 7 T) of an agar phantom containing untreated IGROV-1 cells (1) or cells incubated with PLGA-NP-Ctrl (2) or PLGA-NP-Folate (3) for 6 h at 37°C at a 100 μM Gd concentration.

In order to assess whether the combination of Gd/B-NCT and curcumin results in an improvement of the treatment outcome (with respect to BNCT given as monotherapy), the clinically used B delivery agent boronophenylalanine (BPA) (Figure 8A) was exploited as an alternative B source. For comparison, IGROV-1 cells were incubated for 3h in the presence of increasing BPA concentrations (10-500M B) (Figure 8B). As expected, the internalization of PLGA-NP-Folate (28-220μM B) was significantly more efficient with respect to BPA uptake by IGROV-1 cells and 6.4 μg/g of B was reached after 6h incubation. This amount of B was significantly lower than the minimum B concentration necessary to perform BNCT but since the B was confined within the cells resulted high enough to produce a neutron capture reaction. Only after incubation of BPA at 500 μM B, the concentration of B internalized by cells was 6.4 ug/g whereas for PLGA-NP-Folate was sufficient a five times lower concentration in the incubation medium.

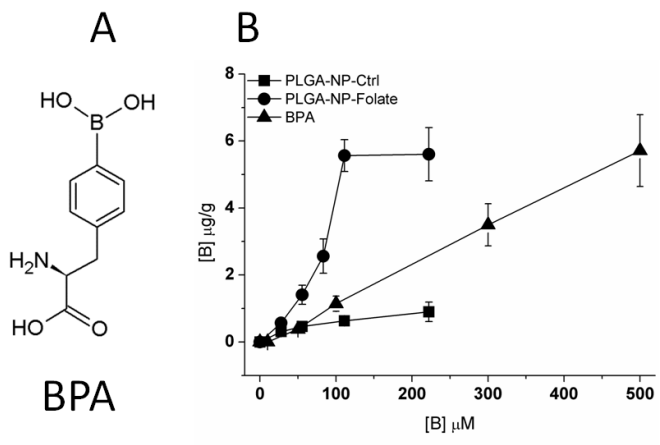

Figure 8: (A) Chemical structure of BPA; (B) B internalization in IGROV-1 cells on incubation in the presence of increasing BPA concentrations (100 – 500 µM B) for 3h at 37°C or with PLGA-NP-Ctrl or PLGA-NP-Folate (28 – 220 µM B) for 6 h at 37°C.

This observation confirmed that the use of targeted nanoparticles allowed the accumulation of B in tumour cells without using huge doses of B carrier; doses that can enhance the non-specific uptake by healthy tissues.

BNCT treatment of IGROV-1 cells. To improve NCT performance, PLGA-NP-Folate were prepared using Gd-DOTAMA and RbCur synthesized with ^{157}Gd (92.3%) and ^{10}B (99 %) enriched isotopes, respectively.

Three groups of IGROV-1 cells were considered: untreated cells irradiated only with thermal neutrons (2); BPA treated cells then irradiated with neutrons (BNCT-group) (4); and PLGA-NP-Folate treated cells then irradiated with neutrons (Gd-BNCT-group) (6) and compared with the not irradiated analogous (1) (3) (5), respectively. Under these conditions both treated cell groups internalized the same amount of ^{10}B (6.4 µg/g).

Groups (2), (4) and (6) were irradiated for 15' in the thermal column of the TRIGA Mark II reactor at the University of Pavia (Reactor Power 30kW).

IGROV-1 cells treated with PLGA-NP-Folate (5-6) and BPA (3-4) were incubated for 6h with PLGA-NP-Folate (130µM B) and 3h with BPA 500µM B, respectively. Figure 9A shows the percent of cells that survived to neutron irradiation (2,4,6) with respect the non-irradiated groups (1,3,5). We can observe that the number of viable cells was significantly lower in the case of cells internalizing PLGA-NP-Folate (6), with respect cells internalizing BPA (4) (with the same ^{10}B amount), both irradiated with neutrons as a consequence of the additional cytotoxic effect of curcumin. Whereas the difference between group 5 and 6 is less evident and not significant. Interestingly, the results changed by considering the proliferation rate of cells surviving to irradiation (Figure 9B). Figure 9B shows that both cells not irradiated (3) and irradiated (4) after BPA treatment, together with cells treated with PLGA-NP-Folate (without irradiation) (5) restart to proliferate rapidly, 72 h after the irradiation, as the untreated controls (1). On the contrary, cells treated with PLGA-NP-Folate after neutron irradiation (6) showed a complete inhibition of proliferation.

The radiation dose absorbed by cells treated with BPA and PLGA-NP-Folate reaching a ^{10}B concentration of 6.4 µg/g ranges between 4.55 and 4.57 Gy. The total absorbed doses obtained in presence of ^{157}Gd through PLGA-NP Folate increases very modestly of only 0.07% by assuming a non-nuclear Gd accumulation. Anyway, it must be noticed that the 86% of the small increment seen with ^{157}Gd is due to the short range IC and Auger electrons. Consequently, it cannot be excluded that a measurable increment in term of cell death would be visible once the co-localization of ^{157}Gd nuclei and cell DNA is guaranteed. Finally, it is worth to be noticed that in the two NCT groups (cells exposed to BPA or PLGA-NP Folate) about 45% of the total dose is due to the secondary radiations emitted in the neutron capture reaction of ^{10}B while in the third irradiated group (neutron only) receiving about 2.5 Gy, up to 91% of the total dose is imparted by gamma rays coming from the neutron capture reaction of ^{1}H in the cell layer and from the photon background characterizing the irradiation position inside the thermal column.

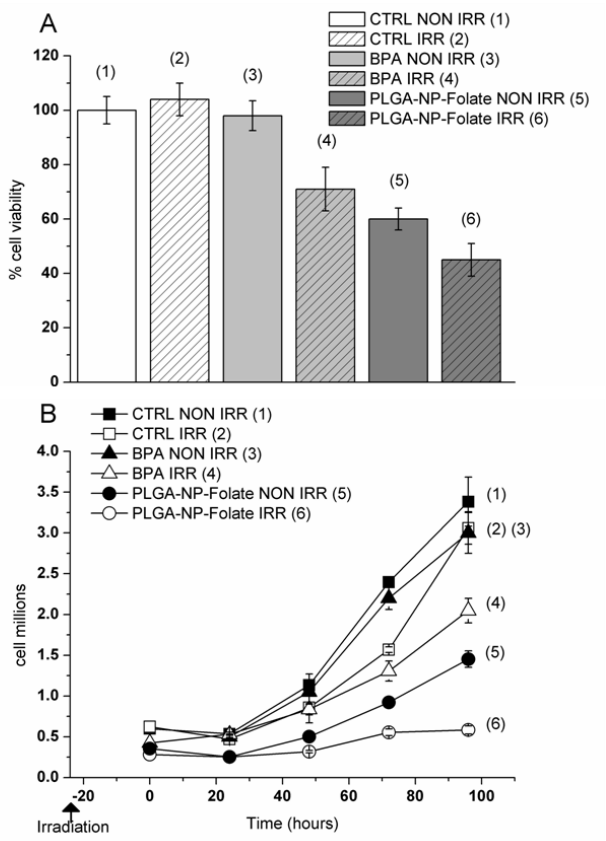

Figure 9: (A) Percentage of IGROV-1 cells that survived the BNCT treatment. (B) Proliferation curves of IGROV-1 cells re-plated one day after the BNCT treatment.

Although ^{157}Gd intracellular concentration was not sufficient to produce an increment in term of cell damage after neutron irradiation, the presence of curcumin before and during the neutron exposure resulted in an improvement of the treatment outcome with respect to BNCT used as monotherapy with the same [B] µg/g accumulated using BPA alone as B source. The presence of curcumin allowed to increase cell mortality and decrease significantly cell proliferation of the surviving cells, despite the B concentration was under the established threshold for an effective BNCT treatment (10-30 µg/g). Due to the difficulties encountered to obtain such high B concentrations, requiring patient perfusion with high concentrated solution of BPA for many hours, this result is fundamental to increase BNCT

competitiveness with respect to the other routine tumor treatment protocols.

Conclusions

In this work, the antitumour activity arising from Gd and B-NCT and curcumin was tested on IGROV-1 ovarian cancer cells, using an innovative folate targeted PLGA nanoparticle containing both Gd and the curcumin-boron complex RbCur. This new nanoparticle has shown to be an efficient carrier by folate receptors and can be exploited for the measurement of Gd and indirectly B concentrations by MRI, opening new perspectives in Neutron Capture applications.

Experimental Session

Curcumin, boric acid, oxalic acid, poly(D,L-lactide-co-glicolide) (PLGA) 50:50 (Resomer RG 503 H), molecular weight (Mw) 30000-60000 Da and Poly(vinyl alcohol) (Mowiol 4-88), Mw 31000 Da were provided by Sigma-Aldrich (St. Louis, Missouri, USA). DSPE-PEG(2000){1,2-distearoyl-sn-glycero-3-phosphoethanolamine-N-[methoxy(polyethylene glycol)-2000] ammonium salt} and DSPE-PEG(2000)folate {1,2-distearoyl-sn-glycero-3 phosphoethanolamine-N-[folate(polyethylene glycol)-2000] ammonium salt} were purchased from Avanti Polar Lipids (Alabaster, AL) The lipophilic Gd-DOTAMA was synthesized according to a previously reported procedure.[22]

Rubrocurcumin synthesis and characterization. A suspension of curcumin (369 mg, 1 mmol), boric acid (62 mg, 1 mmol) and oxalic acid (91 mg, 1 mmol) in 40 mL of toluene was stirred and heated under reflux for 16 hours using a Dean-Stark trap. After cooling, the red precipitate was collected and washed several times with toluene and ethyl acetate before drying under reduced pressure (261 mg, Yield 56%). UV λmax= 545 nm. MS (ESI+): m/z: calcd for $C_{23}H_{19}BO_{10}$ $[M+H]^+$ 466.1; found: 466.9. The compound showed sufficient purity (85%) determined by ^{1}H-NMR spectroscopy, (600 MHz, acetone-d_6) δ 3.93 (s, 6H, OCH3), 6.55 (s, 1H, CH), 6.96 (d, 2H, J= 7.8 Hz, Ar), 7.07 (d, 2H, J= 15.7 Hz, Ar) 7.42 (d, 2H, J= 8.3 Hz, Ar) 7.51 (s, 2H, Ar), 8.11 (d, 2H, J= 15.4Hz, Ar), 8.83 (br, OH). (see supplementary material).

^{1}H NMR spectra were acquired on a Bruker Avance 600 spectrometer (Bruker BioSpin, Ettlingen, Germany). Mass spectral analysis were performed with a Waters 3100 Mass Spectrometer ESI(+) mode.

Synthesis of PLGA nanoparticles. Two different nanospheres were prepared: one targeted with folate and the other non-targeted and used as control. Nanospheres were obtained using the oil-in-water emulsion solvent extraction method. Folate-targeted nanoparticles were prepared dissolving 25 mg of PLGA, 1.2 mg of DSPE-PEG(2000)folate, 1 mg of DSPE-PEG(2000)methoxy, 3.2 mg of Gd-DOTAMA and 6 mg of RbCur in 600 ul (9:1 chloroform:methanol, phase 1); non-targeted nanoparticles were prepared dissolving 25 mg of PLGA, 2.2 mg of DSPE-PEG(2000)methoxy, 3.2 mg of Gd-DOTAMA and 6 mg of RbCur in 600 ul (9:1 chloroform:methanol, phase 1). Phase 2 consisted for both nanoparticles of 3% w/v PVA aqueous solution (3 mL). Phase 1 was added into phase 2 drop by drop and the obtained emulsion was sonicated (Bandelin electronic, Berlin, Germany) in ice at 100% power for 5 minutes. Immediately, the emulsion was put into a rotary evaporator (at 740 mmHg and 30 rpm) for 150 minutes to remove the organic solvent. After the evaporation step, the untrapped compounds were removed by dialysis (molecular weight cut-off of 14000 Da) at 4°C in 1 L of isotonic NaCl/Hepes buffer (HBS). The excess of PVA was removed by washing the emulsion with a vivaspin 20 filter (Sartorius AG, Goettingen, Germany, cut-off of 1 x 10^6 Da). Gd and B amount incorporated in PLGA nanoparticles were measured by inductively coupled plasma mass spectrometry (ICP-MS; element-2; Thermo-Finnigan, Rodano (MI), Italy) after sample digestion performed with concentrated HNO_3 (70%, 1 mL) under microwave heating (Milestone MicroSYNTH Microwave labstation). The amount of Gd was double checked by ^{1}H nuclear magnetic resonance R_1 measurement at 21.5 MHz, 25°C (Stelar Spinmaster, Mede, Italy) of the mineralized complex solution (in 6 mol/L HCl at 120°C for 16 h). The hydrated mean diameter of nanoparticles was determined using a dynamic light scattering (DLS) Malvern Zetasizer 3000HS (Malvern, U.K.) All samples were analyzed at 25°C in filtered (cut-off, 200 nm) HBS buffer (pH 7.4). The amount of RbCur and curcumin loaded into the PLGA-NPs were determined acquiring a UV-VIS spectrum in the range of 360-700 nm in ethanol. According to the calibration curve of RbCur (Y=0.1303X-0.015 (µg/mL at 545nm)) and curcumin (Y=0.15582X (µg/mL at 430nm)) the encapsulation yield was calculated following equation 1:

$$\% \text{ Encapsulation: } (RbCur_{encapsulated} / RbCur_{total}) \times 100 \qquad \text{(Eq. 1)}$$

where: $RbCur_{encapsulated}$ is the amount of RbCur measured after the NP preparation, and $RbCur_{total}$ is the total amount of RbCur used to prepare the NP. Nanoparticles were stored under dark at 4°C until further analysis.

Stability of PLGA nanoparticles. To perform stability test, 2.5 mL of PLGA-NP-Ctrl and PLGA-NP-Folate at a 0.2 mM Gd concentration in HBS buffer, were dialyzed at 37°C (cut-off= 14000 Da) in 40mL HBS for 5 days. At different time intervals, 200uL of the dialyzed NP solution was taken to measure Gd and B concentrations. The 40mL HBS buffer was renewed at each drawing. Gd and B amount were measured by ICP-MS. The experiment was performed in duplicate.

Cell culture and uptake experiments. Human ovarian carcinoma cell line (IGROV-1) was kindly provided by Dr Claudia Cabella (Bracco Imaging, Colleretto Giacosa TO). IGROV-1 cells were cultured in RPMI (Lonza) supplemented with 10% (v/v) FBS, 2 mM glutamine, 100 U mL^{-1} penicillin, and 100 U mL^{-1} streptomycin. Human breast cancer cells (MCF-7) and murine embryo fibroblast cells (BALB/C 3T3) were obtained from the ATCC and NMuMG cell line derived from a healthy mouse mammary gland was kindly provided by Prof. Lollini PL, University of Bologna. MCF-7 were cultured in EMEM (Lonza) supplemented with 10% (v/v) FBS, 2mM glutamine, 100 U mL^{-1} penicillin, and 100 U mL^{-1} streptomycin, 1mM sodium pyruvate and non-essential amino acids, 10 µg/mL insulin (Sigma). NMuMg were cultured in RPMI (Lonza) supplemented with 10% (v/v) FBS, 2mM glutamine, 100 U mL^{-1} penicillin, and 100 U mL^{-1} streptomycin and 10 µg/mL insulin (Sigma). BALB/C 3T3 were cultured in DMEM (Lonza) supplemented with 10% (v/v) FBS, 4mM glutamine, 100 U mL^{-1} penicillin, and 100 U mL^{-1} streptomycin. Cells were incubated at 37 °C in a humidified atmosphere of 5% CO_2. For the *in vitro* uptake experiments, 4.5 × 10^5 of IGROV-1, 6 x 10^5 MCF7, 4 x 10^5 NMumg and 6 x10^5 3T3 BALB/C were seeded in 6 cm diameter culture dishes. After 24h, IGROV-1 medium was removed and it was replaced with RPMI

w/o folate to increase folate receptor expression. After other 24h, all the cells were incubated 6h in folate free medium with increasing concentration (25-200 µM in Gd) of PLGA-NP-Ctrl or PLGA-NP-Folate. At the end of incubation, cells were washed three times with 5 mL ice-cold PBS, detached with 0.05% trypsin and 0.02% EDTA in PBS. IGROV-1 cells were further transferred into glass capillaries for MRI analysis (see below). For the BPA uptake 4.5×10^5 of IGROV-1 were seeded in 6 cm diameter culture dishes. After 48h the medium was removed and replaced with EBSS buffer in the presence of increasing concentrations of BPA (100-500µM B) for 3h. At the end of incubation, cells were washed three times with 5 mL ice-cold PBS, detached with 0.05% trypsin and 0.02% EDTA in PBS. Finally, all cell samples were transferred in falcon tubes and sonicated at 30% of power for 30 sec in ice; their total cell protein concentrations were determined by a commercial Bradford assay (Biorad, Hercules, CA, USA). Gd and B content in the cell samples was determined by ICP-MS and they were normalized by the protein content of each cell sample that was correlated to the number of cells by means of a calibration curve (mg of protein /n° of cells). The µg of B and Gd for g of tissue were thus calculated considering that 1 g of tissue contains $1x10^9$ cells.

MRI. MR images were acquired at 7 T on a Bruker Avance 300 spectrometer equipped with a Micro 2.5 microimaging probe (Bruker BioSpin, Ettlingen, Germany) using a birdcage resonator of 10 mm inner diameter. For recording MR images *in vitro*, cells were pelleted at the bottom of glass capillaries placed in a phantom embedded of high gelling agarose gel (1% w/v in PBS). MR images were acquired using a standard T_1 weighted multislice spin echo sequence, using the following parameters: TR/TE/NEX 250/4/6, resolution 78 µm, slice thickness 1 mm.

Cell irradiation. Eight flasks, three with IGROV-1 cells previously incubated for 6h in the presence of PLGA-NP-Folate, 130 µM B, three incubated for 3h with BPA at 500 µM B concentration and two non-treated control cells were irradiated in the thermal column of the TRIGA Mark II reactor at the University of Pavia, Italy. Cells incubated in the presence of PLGA nanoparticles and BPA were washed with cold PBS before irradiation. At the end of the irradiation, the medium was removed, it was replaced with fresh RPMI and flasks were placed at 37 °C in a humidified atmosphere of 5% CO_2.

The irradiation position was previously characterized from the point of view of neutron flux distribution by means of thin activation foils.[34] At a reactor power of 250 kW the thermal neutron flux in air at that position is $(1.20 \pm 0.10) \times 10^{10}$ cm^{-2} s^{-1}, while the epithermal and fast components are at least two orders of magnitude lower. The flux is roughly constant (less than 1%) along the vertical direction, thus the flasks were superposed and irradiated at the same time. The irradiation time has been fixed at 15 minutes at a reactor power of 30 kW, corresponding to a thermal neutron fluence of 1.30×10^{12} cm^{-2}

Proliferation assay. The day after irradiation cells were detached with 0.02% EDTA and the trypan blue exclusion test of cell viability was performed. Then, around 6×10^5 IGROV-1 cells from each differently treated flask were seeded in 10 cm diameter culture dishes. After 1, 2, 3 and 4 days, cells were washed with PBS, detached with 0.05% trypsin and 0.02% EDTA in PBS and transferred into falcon tubes. Then, cells were sonicated for 30 sec at 30% power in ice and the total cell protein concentration from cell lysates was determined by the Bradford method, using bovine serum albumin as a standard.

Acknowledgements.

This research was funded by MIUR (PRIN 2012 code 2012SK7ASN), the AIRC investigator Grant IG2013 and by the National Institute of Nuclear Physics (INFN), Italy, project "NETTUNO". This research was performed in the framework of the EU COST Action TD1004. The authors would like to thank the staff of the Laboratory of Applied Nuclear Energy (L.E.N.A.), University of Pavia, for their precious support during the realization of neutron irradiations.

Keywords: Gadolinium and Boron Neutron Capture Therapy, Magnetic Resonance Imaging, Curcumin, PLGA, Oncology.

References.

[1] J. A. Kemp, M. S. Shim, C.Y. Heo, Y. J. Kwon, *Adv. Drug. Deliv. Rev*. **2015**, pii: S0169-409X(15)00244-6.

[2] H. E. Barker, J. T. Paget, A. A. Khan, K. J. Harrington, *Nat. Rev. Cancer* **2015**, *15*, 409-425.

[3] L. Gatti, F. Zunino, *Methods Mol. Med*. **2005**, *111*, 127-148.

[4] A. H. Soloway, W. Tjarks, B. A. Barnum, F. G. Rong, R. F. Barth, I. M. Codogni, J. G. Wilson, *Chem. Rev.* **1998**, *98*, 1515-1562.

[5] a) E. C. C. Pozzi, J. E. Cardoso, L. L. Colombo, S. Thorp, A. Monti Hughes, A. J. Molinari, M. A. Garabalino, E. M. Heber, M. Miller, M. E. Itoiz, R. F. Aromando, D. W. Nigg, J. Quintana, V. A. Trivillin, A. E. Schwint, *Radiat. Environ. Biophys*, **2012**, *51*, 331-339; b) N. S. Hosmane, J. A. Maguire, Y. Zhu, M. Takagaki, *Boron and Gadolinium Neutron Capture Therapy for Cancer Treatment*, World Scientific Pub Co Inc, Singapore, **2012**.

[6] a) R. F. Barth, *Appl Radiat Isot*. **2009**, *67*, S3-6; b) R. F. Barth, J. A. Coderre, M.G. Vicente, T. E. Blue, *Clin. Cancer Res*. **2005**, *11,* 3987-4002; c) M. F. Hawthorne, M. W. Lee, *J. Neurooncol*. **2003**, *62*, 33-45

[7] a) T. Kageji, S. Nagahiro, Y. Mizobuchi, K. Matsuzaki, Y. Nakagawa, H. Kumada, *J. Med. Invest.* 2014*, 61*, 254-263; b) C. M. van Rij, A. J. Wilhelm, W. A. Sauerwein, A. C. van Loenen, *Pharm. World Sci.* 2005, *27*, 92-95; c) T. Yamamoto, K. Nakai, A. Matsumura, *Cancer Lett.* **2008**, *262*, 143-52.

[8] a) Y. W. Liu, C. T. Chang, L. Y. Yeh, L. W. Wang, T. Y. Lin, *Appl. Radiat. Isot.* **2015**, *106*, 121-124; b) T. Aihara, N. Morita, N. Kamitani, H. Kumada, K. Ono, J. Hiratsuka, T. Harada, *Appl. Radiat. Isot.* **2014**, *88*, 12-15; c) L. Kankaanranta, T. Seppälä, H. Koivunoro, K. Saarilahti, T. Atula, J. Collan, E. Salli, M. Kortesniemi, J. Uusi-Simola, P. Välimäki, A. Mäkitie, M. Seppänen, H. Minn, H. Revitzer, M. Kouri, P. Kotiluoto, T. Seren, I. Auterinen, S. Savolainen, H. Joensuu, *Int. J. Radiat. Oncol. Biol. Phys*. **2012**, *82*, e67–e75.

[9] P. R. Menéndez, B. M. Roth, M. D. Pereira, M. R. Casal, S. J. González, D. B. Feld, G. A. Santa Cruz, J. Kessler, J. Longhino, H. Blaumann, R. Jiménez Rebagliati, O. A. Calzetta Larrieu, C. Fernández, S. I. Nievas, S. J. Liberman, *Appl. Radiat. Isot.* **2009***, 67*, S50-53.

[10] R. F. Barth, M. G. Vicente, O. K. Harling, W. S. 3rd Kiger, K. J. Riley, P. J. Binns, F. M. Wagner, M. Suzuki, T. Aihara, I. Kato, S. Kawabata, *Radiat. Oncol.* **2012**, *7*, 146-167.

[11] a) V. M. Ahrens, R. Frank, S. Boehnke, C.L. Schütz, G. Hampel, D. S. Iffland, N. H. Bings, E. Hey-Hawkins, A. G. Beck-Sickinger, *ChemMedChem* **2015**, *10*, 164-72; b) S. Tachikawa , T. Miyoshi, H. Koganei, M. E. El-Zaria, C. Viñas, M. Suzuki, K. Ono, H. Nakamura, *Chem Commun*. **2014**, *50*, 12325-12328.

[12] a) G. S. Spicer, J. D. H. Strickland, ***J. Chem. Soc.*** **1952**, 4644-4650; b) Z. Sui, R. Salto, J. Li, C. Craik, P. R. Ortiz de Montellano, *Bioorg Med Chem*. **1993**, *1*, 415-422.

[13] a) T. Esatbeyoglu, P. Huebbe, I. M. Ernst, D. Chin, A. E. Wagner, G. Rimbach, *Angew. Chem. Int. Ed. Eng.* **2012**, *51*, 5308-5332; b) B. B. Aggarwal, C. Sundaram, N. Malani, H. Ichikawa, *Adv Exp Med Biol*. **2007**, *595*, 1-75.

[14] a) M. López-Lázaro, *Molecular Nutrition and Food Research* **2008**, *52*, S103-S127; b) A. Sahebkar, A. F. Cicero, L. E.

Simental-Mendía, B. B. Aggarwal, S. C. Gupta. *Pharmacol Res*. **2016**, *107*, 234-42.
[15] a) G. C. Jagetia, *Adv. Exp. Med. Biol.* **2007**, *595*, 301-320; b) D. Chendil, R.S. Ranga, D. Meigooni, S. Sathishkumar, M.M. Ahmed, *Oncogene* **2004,** *26,* 1599-607.
[16] C. Syng-Ai, A. L. Kumari and A. Khar, *Mol. Cancer Ther*. **2004**, ***3***, 1101-1108.
[17] a) M.R. Hayes, J. Metcalfe, *Analyst* **1962**, *87*, 956-969; b) J.W. Jr. Mair, H. G. Day, *Anal Chem*. **1972**, *44*, 2015-2017; c) W. W. Choi, K. Y. Chen, *American Water Works Association* **1979**, *71*, 153-157; d) M. A. Wimmer, H. E. Goldbach, *J. Plant Nutr. Soil Sci*. **1999**, *162*, 15-18; e) S. Wanninger, V. Lorenz, A. Subhan, F. T. Edelmann, *Chem. Soc. Rev.* **2015**, *44*, 4986-5002.
[18] a) S. Wanninger, V. Lorenz, A. Subhan, F. T. Edelmann, *Chem. Soc. Rev*. **2015**, *44*, 4986-5002; b) S. Banerjee, A. R. Chakravarty, *Acc. Chem. Res.* **2015**, *48*, 2075-2078.
[19] M. Z. Ahmad, S. A. Alkahtani, S. Akhter, F. J. Ahmad, J. Ahmad, M. S. Akhtar, N. Mohsin, B. A. Abdel-Wahab. *J. Drug Target* **2016**, *24*, 273-293.
[20] M. K. Pandey, S. Kumar, R. K. Thimmulappa, V. S. Parmar, S. Biswal, A. C. Watterson, *Eur. J. Pharm. Sci.* **2011**, *43*, 16-24.
[21] a) R. A. Jain, Biomaterials **2000**, 21, 2475-2490; b) R. N. Mariano, D. Alberti, J. C. Cutrin, S. Geninatti Crich, S. Aime, *Mol Pharm*. **2014**, *11*, 4100-4106; c) L. N. Turino, R. N. Mariano, S. Boimvaser, J. A. Luna, *J. Pharm. Innov*. **2014**, *9*, 132–140.
[22] P. L. Anelli, L. Lattuada, V. Lorusso, M. Schneider, H. Tournier, F. Uggeri, *Magma* **2001**, *12*, 114−120.
[23] a) S. Geninatti-Crich, A. Deagostino, A. Toppino, D. Alberti, P. Venturello, S. Aime, *Anticancer Agents Med. Chem.* **2012**, *12*, 543-553; b) K. Takahashi, H. Nakamura, S. Furumoto, K. Yamamoto, H. Fukuda, A. Matsumura, Y. Yamamoto, *Bioorg. Med. Chem.* **2005**, *13*, 735-743; c) K. B. Gona, V. Gómez-Vallejo, D. Padro, J. Llop, *Chem. Commun. (Camb)* **2013**, *49*, 11491-11493.
[24] a) N. Cerullo, D. Bufalino, G. Daquino, *Appl. Radiat. Isot*. **2009**, *67*, S157-160; b) N. Protti, S. Geninatti-Crich, D. Alberti, S. Lanzardo, A. Deagostino, A. Toppino, S. Aime, F. Ballarini, S. Bortolussi, P. Bruschi, I. Postuma, S. Altieri, H. Nikjoo, *Radiat. Prot. Dosimetry* **2015**, *166*, 369-373.
[25] a) F. Yoshida, T. Yamamoto, K. Nakai, A. Zaboronok, A. Matsumura, *Appl. Rad. Isot.* **2015**, *106*, 247-250; b) A. Matsumura, T. Zhang, K. Nakai, K. Endo, H. Kumada, T. Yamamoto, F. Yoshida, Y. Sakurai, K. Yamamoto, T. Nose, *J. Exp. Clin. Cancer Res.* **2005**, *24*, 93-98; c) D. Alberti, N. Protti, A. Toppino, A. Deagostino, S. Lanzardo, S. Bortolussi, S. Altieri, C. Voena, R. Chiarle, S. Geninatti Crich, S. Aime, *Nanomedicine* **2015***, 11*, 741-750; d) C. Salt, A. J. Lennox, M. Takagaki, J. A. Maguire, N. S. Hosmane, *Russ. Chem. Bull*. **2004**, *53*, 1871-1888.
[26] A. Deagostino, N. Protti, D. Alberti, P. Boggio, S. Bortolussi, S. Altieri, S. Geninatti-Crich, *Future Med. Chem.* **2016**, *8*, 899-917.
[27] S. K. Sahooa, J. Panyama, S. Prabhaa, V. Labhasetwara, SS. Jalisatgi *J. Controlled Release* **2002**, *82*, 105−114.
[28] S. W. Choi, H. Y. Kwon, W. S. Kim, J. H. Kim, *Colloids Surf*. **2002**, *201*, 283−289.
[29] A. Kumari, S.K. Yadav, S.C. Yadav, *Colloids Surf. B. Biointerfaces* **2010**, *75*, 1-18.
[30] a) D. Alberti, M. van't Erve, R. Stefania, M. R. Ruggiero, M. Tapparo, S. Geninatti Crich, S. Aime, *Angew. Chem. Int. Ed. Engl.* **2014**, *53*, 3488-3491; b) U. M. Le, Z. Cui, *Int. J. Pharm.* **2006**, *312*, 105-112
[31] D. Feng , Y. Song , W. Shi, X. Li , H. Ma, *Anal Chem.* **2013**, 85, 6530-5
[32] a) B. Stella, S. Arpicco, M.T. Peracchia, D. Desmaële. J Hoebeke, M. Renoir, J. D'Angelo, L. Cattel, P. Couvreur, *J. Pharm Sci.* **2000**, 89,1452-64; b) Y. Lu, P.S. Low, *Adv. Drug Deliv. Rev.* **2002**, 54, 675-693
[33] F. Sonvico, C. Dubernet, V. Marsaud, M. Appel, H. Chacun, B. Stella, M. Renoir, P. Colombo, P. Couvreur, *J. Drug Del. Sci. Tech.*, **2005**, 15, 407-410.
[34] N. Protti, S. Manera, M. Prata, D. Alloni, F. Ballarini, A. Borio di Tigliole, S. Bortolussi, P. Bruschi, M. Cagnazzo, M. Garioni, I. Postuma, L. Reversi, A. Salvini, S. Altieri, *Health Phys.* **2014**, *107*, 534-541.

Entry for the Table of Contents

"Theranostic" Nanoparticles loaded with imaging probes and rubrocurcumin for a combined cancer therapy.

*Diego Alberti, Nicoletta Protti, Morgane Franck, Rachele Stefania, Silva Bortolussi, Saverio Altieri, Annamaria Deagostino, Silvio Aime, Simonetta Geninatti Crich**

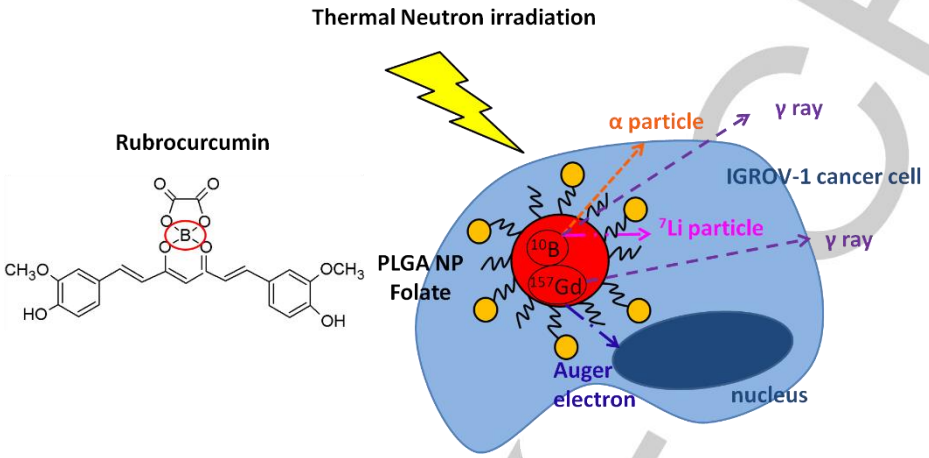

Innovative theranostic agent based on folate targeted PLGA nanoparticles loaded with a boron-curcumin complex (Rubrocurcumin) and the MRI contrast agent Gd-DOTAMA to combine BNCT with the anti-cancer activity of curcumin for the imaging guided treatment of human ovarian cancer cells (IGROV-1).